

Scaffolds for drug delivery, part I: electrospun porous poly(lactic acid) and poly(lactic acid)/poly(ethylene oxide) hybrid scaffolds

Sara Honarbakhsh · Behnam Pourdeyhimi

Received: 19 August 2010/Accepted: 6 December 2010/Published online: 16 December 2010
© Springer Science+Business Media, LLC 2010

Abstract This is the first in a series of papers, focused on the development of a biodegradable, controlled, and potentially targeted drug delivery system. In this paper, we describe the production of highly porous biodegradable fibrous structures suitable for biomedical applications and as a matrix for drug delivery. Two structures are described below. The first structure is composed of electrospun poly(lactic acid) (PLA) fibers and is unique due to (1) the uniformity of its constituent fibers' diameter, (2) consistent surface pore dimensions of each fiber, (3) the use of only a single solvent, (4) interior nano-size porosity throughout each individual fiber, and (5) the independency of surface pore dimensions on fiber diameter. The produced matrix will be further impregnated with cargo loaded nanoparticles—*Red clover necrotic mosaic virus* (RCNMV)—to achieve a controlled drug delivery system (described in Part III) for cancer treatments. Such a structure can also be used as tissue engineering scaffolds and filter media. The second electrospun structure has enhanced hydrophilicity compared to PLA matrix and is formed by blending poly(lactic acid)/poly(ethylene oxide) (PEO) polymers. The incorporation of PEO in the matrix introduces preferable sites for aqueous compounds to be attached to while retaining the overall structural integrity and porous morphology. It is hypothesized that the existence of alternative hydrophilic and hydrophobic segments in the structure may

reduce post-implantation complications such as platelet adhesion.

Introduction

Nano/micro-scale polymeric structures are one of the most promising structures in drug delivery due to their ability to provide a matrix capable of hosting and protecting drug carriers and the drugs themselves against chemical and physiological triggers. Providing that biodegradable components are incorporated in the matrix structure, controlled drug release profile will be achievable by taking advantage of altering their degradation rate and swelling profile [1, 2].

“Controlled drug delivery” using a polymeric system is meant to indicate that the release of the drug—in the polymeric matrix—occurs in a predetermined manner so that the potential for both under and overdosing is eliminated. The release can be either immediate, or constant, or cyclic or even triggered by the surrounding environment [3].

One of the most straightforward and reproducible methods for making polymeric fibers is electrospinning [1, 4]. In this process, fibers in the tens of nanometers to tens of micrometers diameter range are producible.

There are many parameters affecting the morphology of the electrospun fibers, broadly categorized into polymer solution parameters, processing, and ambient conditions [1, 2]. The resultant structure can be made up of beads, solid fibers, hollow fibers, porous fibers, and so forth among which, porous fibers are of great interest. Porous structures, owing to their large specific surface area coupled with high porosity, are believed to facilitate drug diffusion and improve the structure's fluid transport. By controlling the porosity of the matrix and the diameter of

S. Honarbakhsh (✉) · B. Pourdeyhimi
The Nonwovens Cooperative Research Center, The Nonwovens Institute, North Carolina State University, Raleigh, NC 27695-8301, USA
e-mail: shonarb@ncsu.edu

B. Pourdeyhimi
e-mail: bpourdey@ncsu.edu

individual fibers, a zero-order release profile will be potentially achieved [5]. Obtaining a steady release of the drug is advantageous as the release rate will be independent of the remaining drug in the drug carrier and its composition [6, 7]. The only driving factor determining the release rate will thus be the geometry of the fibers and/or pores and the structure's surface area. In other words, by designing a matrix that not only is capable of hosting drug loaded nanocarriers but also inherits uniform fibers possessing surface pores with consistent dimensions, controlled release of the impregnated drug will be possible.

The surface area of a fiber can be greatly increased when its structure is switched from solid to porous. There have been many approaches in order to produce electrospun fibers with controllable surface pore dimensions [8]. Two slightly different approaches have been reported so far for introducing porosity into the bulk of an electrospun fiber. One is based on the selective removal of a component from fibers made of a composite or blend material whereas the other one involves the use of phase separation of different polymers or between polymer(s) and solvent(s) during electrospinning [3, 9–19].

In a different approach, Park et al. investigated the effect of adding a second solvent to produce porous electrospun fibers. They have shown that by adding a second solvent with a higher vapor pressure compared to the primary solvent, a binary system is created in which the solvent with higher volatility evaporates rapidly during electrospinning process and pores are formed on the fiber surface [20].

One of the challenges in producing porous fibers is the degree to which the pore size and distribution can be controlled without adversely affecting the fiber properties. It has been shown that there is a direct relationship between fiber diameter and pore diameter: a smaller fiber will naturally result in smaller pores [4].

In the approach presented below, we will demonstrate that by incorporating only a single highly volatile solvent, unique porous fibrous structures are possible in a one-step process. The distinguishing factor here is the ability to produce a range of fiber diameters while more or less maintaining pore dimensions. Fortunately, the resultant fibers appear to have porous interiors throughout their entire length.

Poly(lactic acid) (PLA) is a FDA approved and widely used material in drug delivery applications due to its biocompatibility and biodegradability, adequate mechanical strength, and thermal stability. As an aliphatic polyester, PLA contains flexible ester bonds and degrades through the hydrolysis of the backbone ester group into non-toxic matter in solutions of various pH levels [21, 22].

PLA is however, rather hydrophobic and needs to be modified in order to obtain a structure capable of

interacting with aqueous drug compositions while retaining its unique morphology and structural integrity. Both bulk and surface modification approaches have been reported for enhancing PLA hydrophilicity [23, 24]. In bulk modification, either lactide is co-polymerized with functional groups and monomers (such as malic acid, PEO, Dextran) or a hydrophilic polymer (such as PEO), is incorporated into the electrospinning solution. Note that there is an optimal concentration level for PEO with respect to dissolution of PEO in presence of an aqueous medium. Also, the viscosity of the spinning solution decreases considerably which may adversely affect the electrospinning process.

In surface modification strategies, polar groups (such as hydroxyl, carboxyl, and other oxygen functional groups) emerge on the surface. The techniques include radio frequency (RF) plasma treatment in O₂, oxygen radio frequency glow discharge (RfGD), plasma graft polymerization, UV/O₃ irradiation, and so forth [25–28].

Like PLA, PEO is one of the polymers of choice as it is a biodegradable hydrophilic polymer. It has been demonstrated that it can be incorporated into the electrospinning solution. PEO degrades by the hydrolysis of its ester and amide bonds, it is nontoxic and also it is approved by FDA (for use as carriers in different pharmaceutical formulations [29]).

Below, we demonstrate how tunable fiber diameters with uniform pore dimensions and a porous interior can be produced by using PLA and PLA/PEO blends. The ability of producing surface pores dimensionally independent of the fiber diameter in addition to the existence of interior nano-size channels throughout the fiber length provide opportunities in a myriad of critical applications such as tissue engineering, fluid flow, absorption, and creating a matrix for hosting therapeutic agents. These unique structures are obtained in a one-step process using only one solvent without the need for any post-treatments.

Materials and methods

Poly(lactic acid) (PLA) was obtained from Nature Works LLC and was used as received. Dichloromethane (DCM) was obtained from Sigma-Aldrich Co. Solutions of different PLA concentrations (0.8, 3, 5, and 10 wt%) dissolved in DCM were prepared and stirred at room temperature until a homogenous solution was achieved. Poly(ethylene glycol) (PEO) (M_w 200 K) was purchased from Scientific Polymer Products INC. Blend solutions (70/30, 80/20, and 90/10 wt%) of PLA and PEO dissolved in DCM (total polymer concentration of 12 wt%) were prepared and electrospun in order to produce the hybrid matrices with enhanced hydrophilicity.

A variable high voltage supply (Gamma High Voltage Research, positive polarity) was used for inducing the charge to the solution contained in a 10 mL syringe which was pumped (Pump 11, Harvard Apparatus) with a tunable flow rate. A 5 cm long needle with internal diameter of 0.5 mm was attached to the syringe and it was connected to the power supply. The collector plate, located at a distance of 10 cm distance, was grounded and placed in front of the syringe.

Field emission scanning electron microscopy (SEM JEOL 6400 F) and focused ion beam (FEI Quanta 200 3D FIB System) were used to characterize the electrospun structures. To reduce charging, the samples were coated with Au prior to taking SEM images. To protect the sample in FIB, platinum strip was deposited on top of the sample. The image analysis measurement tool on the JEOL software was used for dimension measurements. 10 fibers (five images) and 30 pores (two images) were used to obtain the average diameter of the fibers and pore dimensions. Static water contact angles of the webs were measured according to the drop method using a zoom lens connected to a CCD camera. The contact angle between the deionized water droplet and web surface was measured using Image Software developed at The Nonwovens Cooperative Research Center.

Surface area measurements (S_{BET}) were obtained by using the multi-point BET method. The samples (weighting at least 0.189 g each) were compressed and held on the bottom of the sample holder by using a glass rod during the test. The total pore volume (V_p), pore distribution and the porosity of the structures were calculated by using Liquid Extrusion Porosimetry technique.

Results and discussion

All PLA electrospun structures, except for the webs produced from 10 wt% PLA/DCM solutions, contained extensive beaded structures (Fig. 1). Interestingly, the beads were all porous but no preferred pattern was evident.

However, when PLA concentration was set to 10 wt%, uniform unperturbed networks of porous fibers was achieved (Fig. 2). Table 1 summarizes the voltage and flow rate ranges used.

The fibers had uniform diameters and no fiber–fiber fusion was observed at cross-over points probably because of the high volatility of the DCM solvent. However, one may obtain fused (or collapsed) fibers if the gap between the needle and collector plate is too small which will in turn prevent complete evaporation of the solvent prior to



Fig. 1 SEM images of non-fibrous electrospun structures: **a** 0.8, **b** 3, and **c** 5 wt% PLA/DCM, *scale bars* = 5, 10, 10 μm , respectively

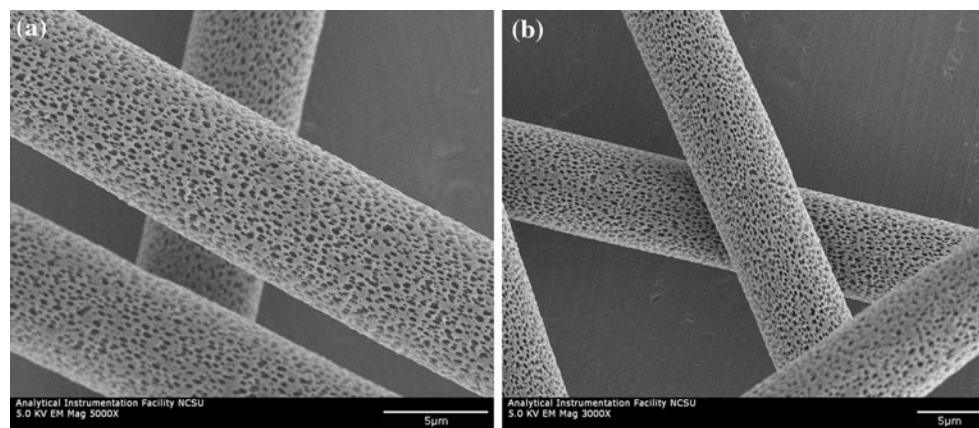


Fig. 2 **a, b** SEM images of PLA electrospun fibers, *scale bars* = 5 μm

Table 1 Electrospinning conditions for 10 wt% PLA/DCM solutions

Sample number	Voltage (kV)	Flow rate (mL/min)
A-1	8	0.5
A-2	8	0.7
A-3	8	1
A-4	8	2
A-5	8	3
B-1	10	0.7
B-2	10	1
B-3	10	2
B-4	10	3
C-1	12	0.5
C-2	12	1
C-3	12	2
C-4	12	3

fiber solidification and deposition. The elliptical pores dimensions were consistent with their major axis elongated along the fiber axis due to the drawing effect on the fibers during electrospinning. Table 2 shows the fibers and their surface pores dimensions for the minimum and maximum voltage and flow rate used.

Increasing the flow rate results in larger fibers as expected. Increasing the voltage on the other hand, decreases the fiber diameter. This is due to the increased

repulsive electrical force which further elongates the fiber. The dimensions of the pore, however, remain fairly consistent regardless of electrospinning conditions and fiber size; that is regardless of fiber diameter, the pores possess consistent diameter both in their major axis and minor axis. This unique characteristic is most beneficial when considering the produced structure in fluid flow and cell attachment applications [8]. By changing environment humidity, electrospinning speed (air flow over the traveling jet), and needle size, one may be able to alter the pores dimensions. However, due to the rapid solvent evaporation rate, increasing the needle size may result in needle clogging and discontinuity in electrospinning.

Further, it was noted that the interiors of the fibers were completely porous throughout the thickness in the form a of nano-size channels elongated through the fiber length (Fig. 3a). In some cases, what appears to be a hollow cavity was also observed along the length of the fiber having the wall thickness of 0.7 μm (Fig. 3b).

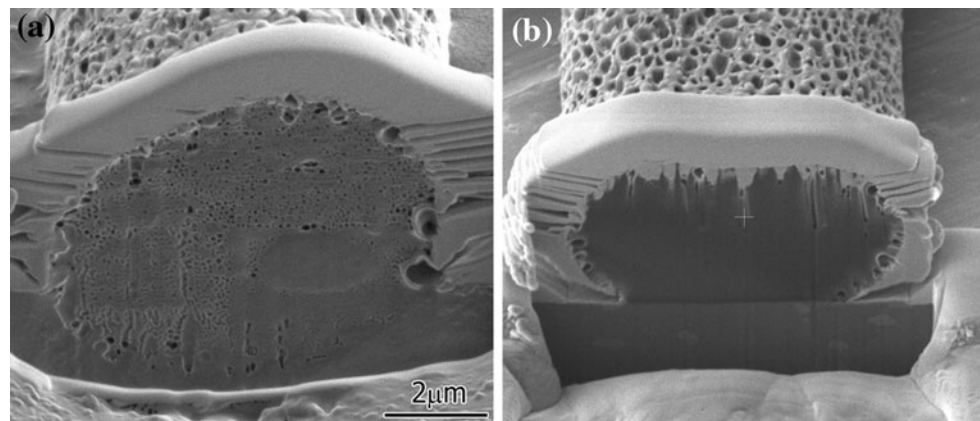
Below, possible mechanisms responsible for pore formation are discussed. The combination of surface and interior porosity of the electrospun fibers are unique.

Pore formation mechanisms

Breath figures, the patterns formed when water droplets condense on a cold surface, is one of the most probable

Table 2 Mean fiber diameter and pore size

Sample number	Mean fiber diameter (μm)	SD	Mean pore major axis (μm)	SD	Mean pore minor axis (μm)	SD
A-1	12	0.2	0.40	0.06	0.23	0.03
A-5	18	0.8	0.48	0.13	0.25	0.09
B-1	7	1.7	0.41	0.05	0.25	0.04
B-4	10	1.7	0.38	0.03	0.17	0.01
C-1	7	0.3	0.37	0.06	0.17	0.02
C-4	12	0.2	0.37	0.05	0.22	0.02

**Fig. 3** a, b PLA electrospun fiber cross-section (images taken using focused ion beam), scale bars = 5 μm

phenomena occurring during electrospinning jet formation which leave behind pore on electrospun fibers surface. For this to happen, there should be a significant temperature difference between the fiber surface and the surrounding media. The solvent used for preparing the electrospinning solution in this study is DCM which is a highly volatile solvent (melting point: -96.7°C , boiling point: 40°C , vapor pressure: 47 kPa at 20°C). The fast evaporation rate further leads to evaporative cooling of the jet/fiber surface during electrospinning process. As the jet surface cools down, the nucleation and growth of moisture in the ambient media is initiated resulting in condensation and growth of moisture in the form of droplets. As the jet dries and the solvent evaporates, the water droplets leave behind imprints on the surface of the fibers in the form of pores [30, 31].

As it is shown in Table 2, the pores appear to have uniform dimensions implying that the condensed water droplets should have been acted as hard spheres on jet surface without any coalescence. Considering the hydrophobic nature of PLA, it can be easily assumed that as water droplets are condensed on fiber surface, they form a circular shape—hard spheres—in order to minimize the interfacial energy between themselves and fiber surface thus leaving behind uniform pores. Moreover, the air flow which is created as the jet travels towards the collector, together with convection currents on the jet surface due solvent evaporation, can potentially create a film of air acting as lubricating medium between the droplets and fiber surface. This can further inhibit the coalescence of neighboring water droplets on fiber surface. In the case of highly volatile solvents such as DCM, it can be assumed that the speed of solvent evaporation is faster than the time needed for two droplets to interact and coalesce [32].

If viewed from a different perspective, fast evaporation of the solvent (evaporative cooling) induces thermally induced phase separation (TIPS) on the fiber surface which explains the occurrence of pores on fiber surface [33, 34]. TIPS results in the formation of polymer-rich and solvent-

rich phases in the fiber. As the solvent evaporates, solvent-rich segments leave behind the pores while polymer-rich segments form the fiber.

On the other hand, radial electrical charge induced on the jet affects the positioning of pores on fiber surface [35, 36]. The charge may not only attract polar water droplets on specified spots on the surface but also aid the solvent to escape through the fiber surface at the spots where it is accumulated. The fact that the charge is induced radially towards the fiber surface may have also influenced the formation of hollow interior.

In a numerical study by Guenthner et al. [37], it was found out that the formation of stable hollow fibers by evaporation takes place only in very small diameter fibers that are subject to extremely rapid drying—common characteristics of electrospinning process. It can, however, be argued that a hollow fiber would either retain its structure or would collapse potentially due to the mechanical stresses on such a structure.

As the solvent evaporates from the interior of the fiber, the outer layer would create a negative gauge pressure (ΔP) at the interior of the fiber which is related to a compressive hoop stress (σ/r) in the outer layer according to $\sigma/r = \Delta P/\Delta R$, r being the average radius of the shell and ΔR being its thickness. It can be immediately concluded that when the skin layer is much thinner than the fiber radius, the stress would be sufficiently large to collapse the fiber. But, that is not the case in the electrospun PLA fibers presented here; the PLA fibers have an interior wall thickness of about $0.7\text{ }\mu\text{m}$ which is significant compared to the fibers size. Thus, we anticipate that there is not going to be a large barrier increase to solvent evaporation which may cause a reduction in diffusion coefficient. Therefore, the wall remains intact and a hollow fiber may be achieved.

Modifying PLA webs hydrophilicity

As it is shown in Fig. 4, the surface morphology of these hybrid PLA/PEO fibers is different from those of PLA

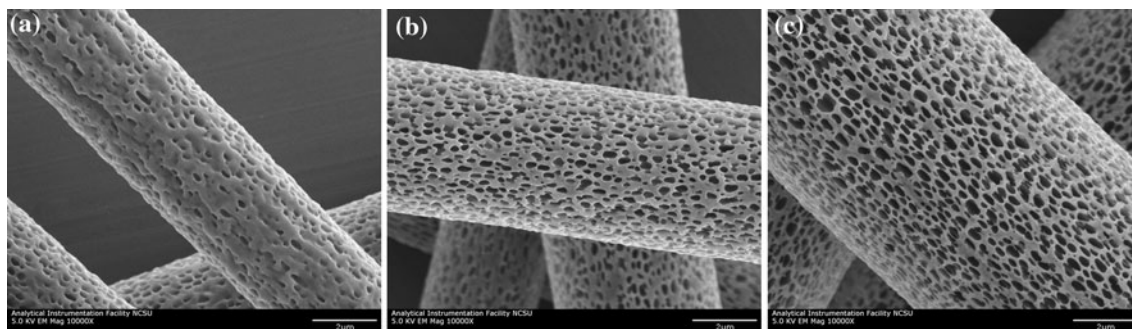


Fig. 4 SEM images of **a** 70/30 wt% PLA/PEO, $F = 0.3\text{ mL/min}$, $V = 12\text{ kV}$; **b** 80/20 wt% PLA/PEO, $F = 0.7\text{ mL/min}$, $V = 10\text{ kV}$; **c** 90/10 wt% PLA/PEO, $F = 0.7\text{ mL/min}$, $V = 10\text{ kV}$, scale bars = $2\text{ }\mu\text{m}$ (F = electrospinning solution flow rate, V = electrospinning voltage)

Table 3 Mean fiber diameter and pore size

Sample composition (wt% PLA/PEO)	Mean fiber diameter (μm)	SD	Mean pore major axis (μm)	SD	Mean pore minor axis (μm)	SD
70/30	5.09	0.86	0.35	0.09	0.20	0.02
80/20	6.12	1.39	0.38	0.15	0.19	0.06
90/10	7.37	1.33	0.37	0.08	0.21	0.05

electrospun fibers. As PEO is a hydrophilic polymer, electrospinning the blend solutions will potentially lead to the formation of fewer surface pores largely due to the coalescence of condensed water droplets on those segments (we hypothesize that the water droplets are absorbed by hydrophilic PEO and spread on the surface). Increasing the weight ratio of PEO will thus be expected to lead to fewer surface pores. Average diameter and surface pore dimensions of 70/30, 80/20 and 90/10 hybrid fibers are presented in Table 3. Apparent decrease in fiber diameter upon increasing PEO content may be mostly due to the increased solution conductivity causing a stronger electrical drag force thus further elongating the fiber along its length.

Contact angle measurements

Figure 5 shows the change of water contact angle due to bulk modification of PLA solution. The measured static contact angle for PLA web is 58.4° while it is 47.71° for 90/10 wt% PLA/PEO webs. 80/20 and 70/30 wt% webs absorb the droplet within a second even in a thick web. As it was expected, by adding PEO to the solution, hydrophilicity of the bulk of the web increases.

Surface area, total pore volume, and porosity

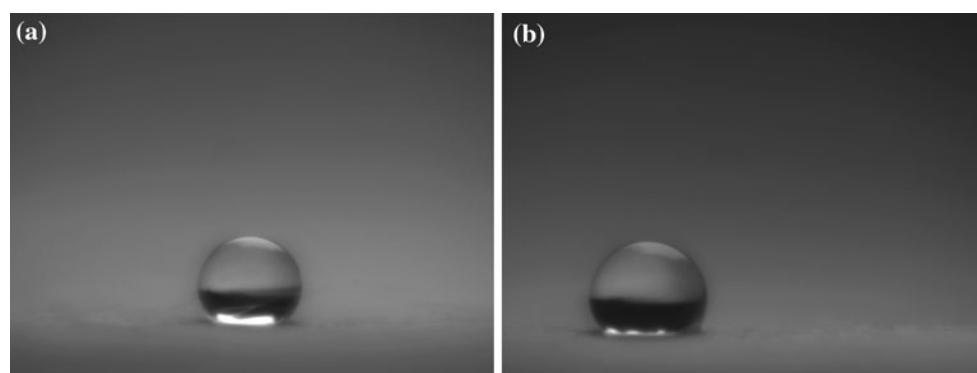
Table 4 summarizes the BET surface area (S_{BET}), total pore volume (V_p), and the porosity of PLA and 70/30 wt% hybrid webs. As previously explained in “Materials and methods” section, PLA webs were obtained from a 10 wt% solution of PLA dissolved in DCM while 70/30 wt% PLA/PEO webs were obtained from a blend solution of PLA

Table 4 BET surface area, total pore volume, and total porosity of PLA and 70/30 wt% PLA/PEO webs

Sample composition	S_{BET} (m^2/g)	V_p (cc/g)	Total porosity (%)
PLA	3.09	30.39	91.18
70/30 wt% PLA/PEO	2.27	29.92	89.78

(70 wt%) and PEO (30 wt%) dissolved in DCM (total blend solution concentration of 12 wt%). Electrospinning conditions for both samples were voltage of 10 kV and 0.7 mL/min flow rate.

PLA electrospun webs exhibit a higher surface area compared to 70/30 wt% PLA/PEO hybrid webs due to their higher porosity. As mentioned earlier, during the electrospinning process, water droplets present in the environment moisture tend to nucleate and condense on fiber surface. Due to higher hydrophobicity of PLA fibers, these droplets retain their spherical shape whereas they coalesce when electrospinning PLA/PEO webs with modified hydrophilicity. Thus, fewer pores are formed on PLA/PEO hybrid structures compared to PLA webs. On the other hand, referring to the total porosity data, one can conclude that the PLA electrospun structures possess larger pores on the fibers and in between individual fibers resulting in a higher total porosity compared to the hybrid structures. This conclusion is further justified in Figs. 6 and 7 which represent intra-fiber pore size distribution of the two samples. As the histograms show, median pore diameter (based on volume) in the PLA web is 52.11 microns while 70/30 hybrid web exhibits a median pore diameter of 22.33 μm .

**Fig. 5** Change in contact angle with the addition of PEO: **a** PLA electrospun web, **b** 90/10 wt% PLA/PEO hybrid electrospun web

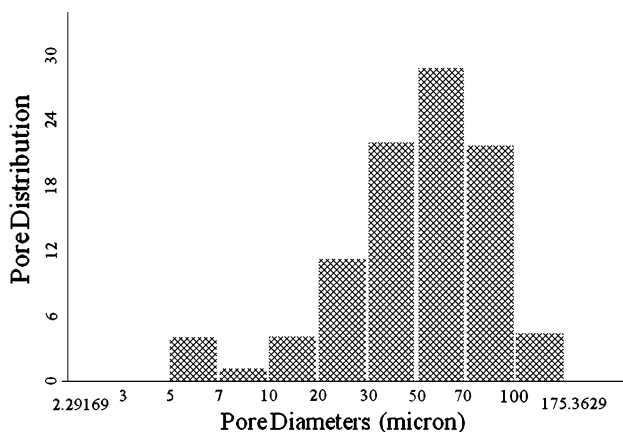


Fig. 6 PLA web pore distribution histogram

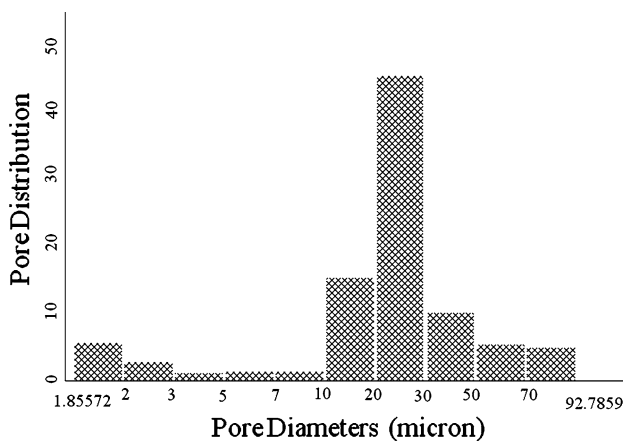


Fig. 7 70/30 wt% PLA/PEO hybrid web pore distribution histogram

Conclusion

Porous structures, with their higher surface area, can act as ideal growth sites of cells and tissues, sites for encapsulating therapeutic agents, pathways for fluid transport and absorption which can be further used in some integral parts of prosthetics, biological filtering media, and so forth. Such structures, if used as a matrix and impregnated with active agents, will also enhance the diffusion of the drug through the pores.

In this study, in order to directly produce a highly porous fibrous structure intended to be used as a drug delivery matrix, solutions of poly(lactic acid) (PLA) dissolved in a highly volatile solvent (dichloromethane (DCM)) were electrospun. The resulting fibers appear to be uniform in diameter and possess surface pores with consistent dimensions as well as porous interior. Fiber diameters of 5–24 μm were produced by altering the electrospinning conditions. Porous fibers (major axis: 0.4 μm, minor axis: 0.2 μm), with both major and minor axis dimensions independent of the fiber diameter, were obtained.

Hybrid structures with enhanced hydrophilicity were also electrospun from blend solutions of PLA and PEO dissolved in DCM. Contact angle decreased from 58.4° for PLA webs to 0° for 70/30 wt% hybrid structures. The produced structures exhibit high porosity values (91.18 and 89.78% for PLA and 70/30 wt% hybrid webs, respectively) while retaining their structural integrity.

The formation of breath figures on the fiber surface, thermally induced phase separation phenomenon (TIPS) as well as the effect of fast solvent evaporation rate, coupled with the radial electrical charge induced to the droplet all may have led to the formation of surface pores and hollow interior in the produced electrospun PLA fibers.

The resultant structures can find applications in drug delivery, filtration, and cell and tissue culture as well as many others requiring high surface area and high transport. In other parts of the series, one such application for drug delivery for chemotherapy will be presented.

Acknowledgements Support for this work was provided by the Nonwovens Cooperative Research Center. Their support of this research is greatly acknowledged.

References

- Kumbar SG, Nukavarapu SP, James R, Hogan MV, Laurencin CT (2008) Recent Pat Biomed Eng 1:68
- Ghasemi-Mobarakeh L, Morshed M, Karbalaie K, Fesharaki M, Naser-Esfahani MH, Baharvand H (2008) Yakhteh Med J 10(3): 179
- Pepps LB (1997) Med Plast Biomater 4:34
- Li D, Xia Y (2004) Adv Mater 16(14):1151
- Leong KF, Chua CK, Gui WS, Verani (2006) Int J Adv Manuf Technol 31:483
- Hughes GA (2005) Nanomedicine 1:22
- Landgraf W, Li NH, Benson JR (2005) Drug Deliv Technol 5(2):48
- Grafe TH, Graham KM (2003) Nanofiber webs from electrospinning. In: The nonwoven in filtration fifth international conference, Stuttgart, Germany
- Frey MW, Li L (2007) J Eng Fibers Fabrics 2(1):31
- Qi Z, Yu H, Chen Y, Zhu M (2009) Mater Lett 63:415
- Gupta A, Saquing CD, Afshari M, Tonelli AE, Khan SA, Kotek R (2009) Macromolecules 42(3):709
- MacCann JT, Marquez M, Xia Y (2006) J Am Chem Soc 128:1436
- Moon SC, Choi JK, Farris RJ (2008) Fibers Polym 9(3):276
- Wu Y, Yu JY, Ma C (2008) Text Res J 78(9):812
- Kim HY, Khil MS, Kim HJ, Jung YH, Lee DR (2003) Preparation of porous filament via electrospinning. In: 2003 Third IEEE conference on nanotechnology, vol 2, p 801
- Jun Z, Hou H, Schaper A, Wendroff J H, Greiner A (2009) Polymers 9
- Jeun JP, Kim YH, Lim YM, Choi LH, Jung CH, Kang PH, Nho YC (2007) J Ind Eng Chem 13(4):592
- Xie J, Li X, Xia Y (2009) Macromol Rapid Commun 29(22):1775
- Han SO, Son WK, Youk JH, Lee TS, Park WH (2005) Mater Lett 59:2998
- Park JY, Han SW, Lee IH (2007) J Ind Eng Chem 13(6):1002
- Cheng Y, Deng S, Chen P, Ruan R (2009) Front Chem China 4(3):259

22. Zhang X, Wyss UP, Pichora D (1994) *J Bioact Compat Polym* 9:80
23. Wang S, Cui W, Bei J (2005) *Anal Bioanal Chem* 381:547
24. Spasova M, Stoilova O, Manolova N, Rashkov I (2007) *J Bioact Compat Polym* 22:62
25. Khorasani MT, Mirzadeh H, Irani S (2008) *Radiat Phys Chem* 77:280
26. Alves CM, Yang Y, Marton D, Carnes DL, Ong JL, Sylvia VL, Deam DD, Reis RL, Agrawal CM (2008) *J Biomed Mater Res B* 87(1):59
27. www.ocw.mit.edu. Accessed Mar 2009
28. Koo G-H, Jang J (2008) *Fibers Polym* 9(6):674
29. www.sigmaaldrich.com. Accessed Mar 2009
30. Briscoe BJ, Galvin KP (1990) *J Phys D* 23:1265
31. Beysens D, Knobler CM (1986) *Phys Rev Lett* 57:1433
32. Srinivasarao M, Collings D, Philips A, Patel S (2001) *Science* 292(5514):79
33. Megelski S, Stephens JS, Chase DB, Rabol JF (2002) *Macromolecules* 35(22):8456
34. Nam YS, Park TG (1999) *J Biomed Mater Res* 47(1):8
35. Ding B, Li C, Miyauchi Y, Kuwaki O, Shiratori S (2006) *Nanotechnology* 17:3685
36. Dayal P, Kyu T (2006) *J Appl Phys* 100(4):043512-1
37. Guenthner AJ, Khombhongse S, Wenxia L, Dayal P, Reneker DH, Kyu T (2006) *Macromol Theory Simul* 15(1):87